Optimizing resource recovery from wastewater with algae-bacteria membrane reactors

Francesca Casagli, Fabrice Béline, Elena Ficara, Olivier Bernard

Optimizing resource recovery from wastewater with algae-bacteria membrane reactors

Francesca Casagli[a], Fabrice Beline[b], Elena Ficara[c], Olivier Bernard[a,*]

[a]: Institut national de recherche en informatique et en automatique (INRIA), Biocore, Univ Cote d'Azur, 2004, Route des Lucioles – BP 93, 06902 Sophia-Antipolis, France

[b]: Inrae, UR OPAALE, 17 Av. de Cucillé, CS 64427, F-35044, Rennes, France

[c]: Dipartimento di ingegneria civile e ambientale (DICA), Politecnico di Milano, 32, Piazza L. da Vinci, 20133 Milan, Italy.

[*]Corresponding author: olivier.bernard@inria.fr

Abstract

Exploiting the combination of algae and bacteria in High Rate Algal/Bacterial Ponds (HRABP) is an emerging approach for wastewater remediation and resource recovery. In this study, the advantage of adding a solid/liquid separation system to uncouple Hydraulic Retention Time (HRT) and Solid Retention Time (SRT) is explored and quantified. A long-term validated model for HRABP was run to simulate and optimize a system at large scale treating digestate. It is shown that by uncoupling HRT and SRT, adapting the liquid depth and the alkalinity content, the algae productivity increases from 9.0-14.5 g m^{-2} d^{-1} (for HRT=SRT in the range of 5 to 10 days) to 20.3 g m^{-2} d^{-1} (for HRT =0.2 d and SRT= 2 d). Simulations pointed out that maximizing the algal productivity or the fraction of recovered nitrogen in the algal biomass are conflicting goals that are achieved under different operating conditions. Conditions maximising the algal productivity favour algae and heterotrophic bacteria while algae and nitrifying bacteria

dominate the system under those conditions optimizing the efficiency of nitrogen recycling. Finally, increasing the influent alkalinity and adapting the water depth can boost the algal productivity without meeting conditions favourable to N_2O emission, opening new perspectives for resource recovery through algal biomass valorisation.

Keywords: Wastewater remediation, membranes, process optimization, algae-bacteria, nitrous oxide, emerging pollutants.

1. Introduction

Exploiting the combination of algae and bacteria in High Rate Algal/Bacterial Ponds (HRABP) is an emerging technology for wastewater treatment addressing the most critical aspects of wastewater treatment [1],[2]. Compared to conventional biological processes, HRABP do not need an external oxygen supply, which is known to account for more than 50% of the energy required for wastewater treatment [3]. Recycling nitrogen and phosphorus into the algal biomass is another remarkable opportunity offered by this process [4], since algae can be used as a source of energy or feedstocks [5],[6], *i.e.* with their lipid fraction for biofuels or proteins for bioplastics [7],[8]. Moreover, HRABP have been highlighted for their ability to remove emerging contaminants. These molecules are persistent in the environment, impact on the reproductive systems of aquatic organisms, and bioaccumulate in the food chain [9]. The main emerging pollutants are pesticides, personal care products, pharmaceuticals and flame retardants [6,7]. Conventional wastewater treatment technologies are not designed to remove or degrade these compounds [10], while microalgae have been proven to be a powerful technology for bioremediation of emerging contaminants [5],[12],[13]. Indeed, in the highly oxidizing environment that is achieved thanks to high oxygen levels, microalgae

can catalytically degrade complex compounds, with efficiencies ranging from 30 to 80% for drugs such as ibuprofen, carbamazepine, and caffeine [14],[15],[16],[17]. Combined with bioadsorption and bioaccumulation, the algae process was found to achieve a remarkable removal efficiency for more than 50 emerging contaminants [18].

Adding a separation system, like membrane modules, is a technological breakthrough that leads to the uncoupling of Hydraulic Retention Time (HRT) and Solid Retention Time (SRT). On top of enhancing emerging contaminants removal [6], HRT and SRT separation was shown to considerably enhance the overall process efficiency [19],[20] by increasing microalgal productivity by a factor 3.5 compared to a standard photobioreactor [21] (see the synthesis of various literature studies in Table 1). The key idea is that algal biomass productivity results from the product of net growth rate and biomass concentration which is enhanced when increasing the biomass in the reactor while keeping growth rate at high levels. However, a separation system makes the process more flexible but also more complicated to operate and to optimize by increasing the number of parameters that can be tuned. Concentrating the algae in the system leads to a higher light attenuation and therefore, to a lower growth rate. In such a complex situation, a multi-parametric optimization must be carried out and the guidance of mathematical models has already proven very useful [22],[23]. This is especially decisive in the case of complex dynamical bioprocesses involving a large range of interacting species, like for anaerobic digestion [24].

Recently, the ALBA model (ALBA standing for ALgae-BActeria) was developed and validated. This mathematical model was built to simulate algal-bacterial interactions and competitions in HRABP, to evaluate bioremediation performances and to provide a better understanding of the interactions among the chemical, physical and biological processes. This model was validated and was proven able to accurately predict, under

real outdoor conditions, the complex behaviour of two HRABP pilot-plants operated in two different locations and under different feeding conditions [25],[26]. The model turned out to be accurate in predicting the daily and seasonal responses, even during winter which was never effectively described by previously available models. In total, more than 630 days of pilot-scale experimental data validated the model performance [25],[26] under two different climatic conditions and with the same parameter set. The model confirmed, as experimentally observed [27], that inorganic carbon could become limiting, as a result of the strong competition for inorganic carbon by algae and nitrifiers. It was unexpected that this limitation still happened even under continuous CO_2 injection; the ALBA model revealed that this was due to a shortage in alkalinity owing to the limited alkalinity/nitrogen ratio in the feed, insufficient to support full nitrification. At low alkalinity, inorganic carbon can no more be stored in the medium and becomes limiting both for algae and nitrifiers, leading to conditions favourable to N_2O emission. The high-fidelity ALBA model is therefore a powerful validated tool to assess the process productivity, the nitrogen removal rate, but also the risk of highly impacting N_2O emission.

Table 1: Biomass productivity and nitrogen removarate reported in literature for various outdoor photobioreactors, different influent, HRT, SRT and weather conditions.

Wastewater characteristics (Av ± St.Dev)				Experimental set-up								Performances			Ref
Type	COD [mg L^{-1}]	N-NH_4^+ [mg L^{-1}]	P-PO_4^{3-} [mg L^{-1}]	Reactor type -	Surface [m^2]	Culture depth [m]	HRT [d]	SRT [d]	Duration [d]	Season [-]	Location [-]	Biomass productivity	Unit	N removal rate	unit	
SWW	332±55.0	17.3±8.1	3.9±1.6	raceway + membrane tank	56	0.3	6 4 2.5	6	20 20 20	Spring Spring Autumn	Narbonne	**9.0±0.1** 19.9±0.5 28.5±0.5	gVSS m^{-2} d^{-1}	**1.2±0.2** 2.3±0.4 3.3±0.4	gN m^{-2} d^{-1}	[19]
UWW	577±31.0	97.6±4.6	17.8±1.1	raceway + membrane tank	32	0.12	4.8 3.5 2.6 2 1.8	4.8	N.R.	N.R.	Almeria	**15.2±2.1** 17.0±1.4 22.2±1.6 22.6±1.6 21.9±1.0	gDW m^{-2} d^{-1}	**4.1±0.3** 5.8±0.3 7.0±0.4 8.3±0.3 9.1±0.5	gN m^{-2} d^{-1}	[33]
AnMBR effluent	71.0±35.0	45.0±9.1	4.7±35.0	flat-panel PBRs + membrane tank	2.3	0.25 0.10	1.5	4.5	N.R. 35	N.R Winter	Valencia	15.7±1.4 20.0±2.4	gVSS m^{-2} d^{-1}	2.2±0.4 2.4±0.5	gN m^{-2} d^{-1}	[39]
AnMBR effluent	31.0±5.0	51.3±9.7	6.8±1.6	4 flat-panel PBRs + membrane tank	8.8	0.25	3-4	4.5 9	16 25	N.R. N.R.	Valencia	12.2±1.4 7.7±1.0	gVSS m^{-2} d^{-1}	1.7±0.1 1.3±0.5	gN m^{-2} d^{-1}	[40]
Secondary effluent from WWTP	N.R.	17.8±1.0*	1.6±0.2*	raceway	1.93	0.3 0.15	5 4	5 4	18	Summer	Arcos de la Frontera	26.2±1.2 20.4±1.0	gTSS m^{-2} d^{-1}	0.8±0.1 0.6±0.1	gTN m^{-2} d^{-2}	[41]
Saline SWW	N.R.	N.R.	N.R.	raceway	9.62	0.2	13 8 17 17	13 8 17 17	486	Spring Summer Autumn Winter	South-West France	1.9 3.6 2.0 1.3	gTSS m^{-2} d^{-1}	N.R.	N.R.	[42]
UWW				raceway	8.3	0.05 0.06 0.05 0.05	2.6 2 3.2 3.7	2.6 2 3.2 3.7	46 48 46 41	Spring Summer Autumn Winter	Almeria	25.6 32.7 18.9 12.3	gTSS m^{-2} d^{-1}	96.9 98.7 98.8 97.2	%	[35]
UWW	511±101	75.9±17.7	12.5±5.1**	raceway + greenhouse	80	0.135	10 5 3.3	10 5 3.3	N.R. N.R. N.R.	Spring Summer Autumn Winter Spring Summer Autumn Winter Spring Summer Autumn Winter	Almeria	7.8±4.3 8.5±3.3 7.8±2.8 7.2±3.8 16.1±3.7 25.9±5.1 20.0±4.9 14.2±3.3 13.3±3.9 14.5±3.3 12.5±5.1 11.2±4.9	gDW m^{-2} d^{-1}	N.R. 3.5±0.5 4.3±0.5 3.9±0.2 2.7±0.4 N.R.	gN m^{-2} d^{-1}	[36]
SWW	378±57.2	8.0±2.1	13.0±3.1	raceway	56	0.28	5	5	443	Spring Summer Autumn Winter	Narbonne	18.6±1.7 16.0±5.6 12.4±3.1 12.8±2.4	gTSS m^{-2} d^{-1}	0.5±0.03 0.4±0.10 0.4±0.04 0.3±0.18	gN m^{-2} d^{-1}	[25]
Centrate from UWW	112±34.0	244±79.0	5.7±0.8	raceway	5.78	0.2	9	9	152	Spring, summer, autumn	Milan	5.5±7.4	gTSS m^{-2} d^{-1}	86±7.0	%	[34]
PWW	678±284	195±55.0	19.0±14.0	raceway	3.8	0.2	7-25	7-25	208	Spring, summer, autumn	Milan	**10.7±6.5**	gTSS m^{-2} d^{-1}	**3.9±1.8**	gN m^{-2} d^{-1}	[32]
Centrate from PWW	514±190	310±91.0	13.6±4.0	raceway	3.8	0.2	10 10	10 10	189	Spring Summer	Milan	**10.81±2.16** **12.2±3.5**	gTSS m^{-2} d^{-1}	**5.3±0.6** **6.9±1.3**	gN m^{-2} d^{-1}	[26]

							20	20		Autumn		**6.1±3.1**		**4.9±1.5**		
Simulated Centrate from PWW	514± 190	310±91.0	13.6±4.0	Simulated raceway	2000	0.22	0.2	2	50	Simulated Spring	Simulated Milan	43.1±2.9	gVSS m^{-2} d^{-1}	22.6±12.2	gN m^{-2} d^{-1}	This study
							10	3				19.6±2.1		6.9±0.5		
						0.12	0.2	2				32.0±3.0		12.8±6.8		
							10	3				15.4±2.1		3.7±0.2		
						0.06	1	6				16.2±4.6		10.7±3.3		
							10	3				9.8±1.5		1.9±0.1		

Note. UWW (urban wastewater); AnMBR (anaerobic membrane bioreactor); WWTP (wastewater treatment plant); PWW (piggery wastewater); SWW (synthetic wastewater).

N.R.: Not Reported

*Total nitrogen and total phosphorous values.

**Total phosphorous value

In this work, the ALBA model was upgraded by implementing a solid/liquid separation system to investigate the complex interplay between SRT and HRT. The ALBA model was then validated in this new configuration using the experimental data of Robles et al. [19], carried out in an outdoor pilot reactor. The model was finally used to explore a large range of scenarios, varying HRT, SRT, and liquid depth. The trade-off between algal productivity and nitrogen recycling was explored, while focusing on operating modes that are not susceptible of leading to N_2O emissions.

Finally, the simulation results are deeply discussed and compared with the experimental records reported in literature for outdoor algae-bacteria systems equipped with a separation system, comforting the model prediction and further quantifying the potential of separation systems for wastewater remediation, algae production and nitrogen recycling.

2. Material and methods

2.1. Brief recall of the ALBA model: structure, validation, and implementation

Simulations were run using the high fidelity ALBA model [25], simulating the dynamics of HRABP. The model considers a mixed culture of photoautotrophic algae, heterotrophic bacteria, Ammonium Oxidizing Bacteria (AOB) and Nitrite Oxidizing Bacteria (NOB). In total, it includes 19 biological processes and involves 17 state variables. The biokinetics equations are based on the Liebig's minimum law [28] for limiting elements (carbon, nitrogen and phosphorus), meaning that the most limiting nutrient drives the overall kinetics. Moreover, biokinetics include dependences from light, temperature and pH, since they are the most influencing parameters on microbial dynamics (see SI.1).

The ALBA model embeds an in-depth description of the chemical reactions in the medium resulting in an accurate pH prediction. The pH sub-model is based on dissociation equilibria and mass balances of acids and bases, extending the approach proposed in the ADM1 (Anaerobic Digestion Model n.1 [29],[30]).

The Total Alkalinity (TA) turns out to play an important role in the HRABP dynamics, since it determines the potential of inorganic carbon storage in the bulk. Its expression is defined in terms of molar quantities (mol m^{-3}), as reported in Eq. 2.1.2 [26]:

$$TA = HCO_3^- + 2CO_3^{2-} + H_2PO_4^- + HPO_4^{2-} + 2PO_4^{3-} + OH^- + NH_3 - H^+ - HNO_2 - HNO_3 - H_3PO_4 \quad 2.1.2$$

The CO_2, NH_3, O_2 gas/liquid transfer is also included, quantifying the rate through the global k_La and the diffusivity coefficients.

The model was previously calibrated and validated on two long-term datasets from two pilot-plants, operated under different climatic conditions. The first reactor was a demonstrative-scale raceway of 17 m^3 (with a 56 m^2 surface), located in the South of France (Narbonne area), fed on synthetic municipal wastewater [25]. The second reactor was a pilot-scale raceway of 1 m^3 (with a 3.8 m^2 surface), located in the North of Italy (Milan area), fed on the liquid fraction of piggery digestate [26]. In total, 30 days were used for the calibration phase, while 603 days were exploited for the model validation based on on-line measurements (dissolved oxygen, pH, temperature) and off-line measurements (nitrogen compounds, algal biomass, total and volatile suspended solids, chemical oxygen demand). A more detailed description of the ALBA model, its calibration and validation procedure, can be found in Casagli et al. [25], and summarized in Supporting Information (SI.1 and SI.2).

Other models for describing algae-bacteria system are available in literature, as reviewed in Casagli et al. [26], they can also be modified similarly by introducing a solid/liquid separation term in the hydraulic balance.

The ALBA model was initially developed in AQUASIM and then implemented under MATLAB R2019b. Simulations were run on a PC with 8 i9 vPRO cores. Each simulation took approximately 3 minutes.

2.2. Case study

A theoretical case study was assumed for the optimization exercise, consisting in an industrial HRABP of 2000 m^2 treating digestate, located in the North of Italy (Milan area). Simulations were run focusing on the spring season, where the most affecting environmental conditions (i.e., light and temperature) are closer to the optima for algal growth. The influent was assumed to be a diluted liquid fraction of digestate with the characteristics reported in Table 2 (taken from Pizzera et al., [31]).

Table 2: Influent characteristics and associated model state variables.

Influent characteristics used for the simulations: liquid fraction of piggery digestate			
Description	**Symbol**	**Value**	**Unit**
Total ammoniacal nitrogen	S_{NH}	310.4	gN m^{-3}
Nitrate	S_{NO3}	11.7	gN m^{-3}
Nitrite	S_{NO2}	0	gN m^{-3}
Inorganic soluble orthophosphates	S_{PO4}	13.6	gP m^{-3}
Inorganic carbon	S_{IC}	266.1	gC m^{-3}
Readily biodegradable organic matter	S_S	133.3	gCOD m^{-3}
Inert soluble organic matter	S_I	247.6	gCOD m^{-3}
Inert particulate organic matter	X_I	118.9	gCOD m^{-3}
Slowly biodegradable organic matter	X_S	13.3	gCOD m^{-3}
Dissolved oxygen	S_{O2}	8	gO_2 m^{-3}

Cations	S_{cat}	10	mol m^{-3}
Anions	S_{an}	1e-005	mol m^{-3}
pH	pH	8.5	-
Total alkalinity	TA	500	$mgCaCO_3$ L^{-1}

Note: all the biomasses (X_{ALG}, X_{AOB}, X_{NOB}, X_H) were considered as zero in the influent.

Validated model parameters were taken from Casagli et al. [25]. Only the k_La value was assumed to be lower (10 day^{-1}), which is more similar to an industrial scale application. In all the simulations, the pH was controlled at 7.5 with CO_2 bubbling (see Supp Info SI.3).

2.3. Implementation of HRT and SRT decoupling

The separation system was implemented by imposing a retention factor on all the particulate variables:

$$Ret = \frac{SRT\text{-}HRT}{SRT} = 1\text{-}\frac{HRT}{SRT} = 1\text{-}\alpha \qquad 2.3.1$$

This factor can be positive or negative, depending on the value resulting from the ratio α = HRT/SRT. Consequently, the evolution in time of the particulate variables (X_j) that are retained by the separation system (dX_j/dt [gX_j m^3 d^{-1}]) was implemented in the model as follows:

$$\frac{dX_j}{dt} = \frac{Q_{IN}}{V} \cdot X_{j,\,IN} - \alpha \cdot X_j \cdot \left(\frac{Q_{IN} - Q_{EVAP}}{V}\right) \pm \sum_i v_{i,j}\, \rho_i \qquad 2.3.2$$

where Q_{IN} is the imposed inflow rate [m^3 d^{-1}]; Q_{EVAP} is the outflow leaving the system by evaporation, [m^3 d^{-1}]; V is the reactor volume, [m^3]; $X_{j,IN}$ is the concentration of X_j entering the system with the influent [g m^{-3}]; X_j is the concentration in the system [g m^{-3}]; $v_{i,j}$ is the stoichiometric coefficient associated to the state variable X_j and the process i and ρ_i is the rate of process i [gX_j m^{-3} d^{-1}].

2.4. Optimization study

For the optimization study, 19200 simulations were run, testing the simultaneous influence of different factors on the HRABP performances: i) the HRT (0.2 - 10 d); ii) the SRT (0.2 - 10 d); iii) the liquid depth (δ_L 0.06 - 1 m); and finally, the supplementation of Total Alkalinity (TA, 0 – 12.5 mol m^{-3} added) through dosage of $CaCO_3$.

Simulations were run considering that HRT and SRT could be independently tuned, simulating therefore cases with SRT lower than HRT (biomass harvesting with liquid recirculated in the reactor) or, reversely, HRT lower than SRT (biomass retention).

Algal productivity [gAlg m^{-2} d^{-1}] was defined as:

$$ALG_{productivity} := \frac{X_{ALG} \cdot Q_{out} \cdot \alpha}{S} \cdot \varphi \qquad 2.4.1$$

Where X_{ALG} is the algae concentration in the pond [gCOD m^{-3}]; Q_{OUT} is the outflow, defined as the algebraic sum of Q_{IN}-Q_{EVAP} [m^3 d^{-1}]; S is the reactor surface [m^2]; φ=0.64 is the conversion factor from COD_{ALG} to dry weight (DW) of algae (gDW-Alg.$gCOD^{-1}$).

The efficiency of nitrogen recycling rate was defined as:

$$Eff_{N_{RECYC}}\ [\%] = \frac{Flux_{N_{OUT_{ALG}}}}{Flux_{N_{IN}}} \cdot 100 \qquad 2.4.2$$

Where: $Flux_{Nout,ALG}$ is the mass flow of Nitrogen [gN d^{-1}] in the harvested algal biomass and $Flux_{N,IN}$ is the mass flow of Nitrogen [gN d^{-1}] fed to the HRABP:

$$Flux_{N_{OUT_{ALG}}}\left[\frac{gN}{d}\right] = X_{ALG} \cdot iN_{BM_{ALG}} \cdot Q_{OUT} \cdot \alpha \qquad 2.4.3$$

$$Flux_{N_{IN}} = Q_{IN}\left(S_{NH_{IN}} + S_{NO2_{IN}} + S_{NO3_{IN}} + S_{S_{IN}} \cdot IN_{SS} + S_{I_{IN}} \cdot IN_{SI} + X_{S_{IN}} \cdot iN_{XS} + X_{I_{IN}} \cdot iN_{XI}\right) \qquad 2.4.4$$

where $iN_{BM,ALG}$ is the N content in the algal biomass [gN $gCOD^{-1}$], Q_{IN} is the inflow rate [m^3 d^{-1}]; $S_{NH,IN}$, $S_{NO2,IN}$ and $S_{NO3,IN}$ are the influent concentrations of ammoniacal nitrogen, nitrite and nitrate, respectively [gN m^{-3}]; $S_{S,IN}$, $S_{I,IN}$, $X_{S,IN}$ and $X_{I,IN}$ are influent concentration of the state variables representing the organic matter concentration [gCOD m^{-3}] as soluble degradable, soluble inert, particulate degradable, and particulate inert (I) components, respectively; iN_{SS}, iN_{SI}, iN_{XS} and iN_{XI}, [gN $gCOD^{-1}$] quantify their nitrogen content.

The N recycling efficiency, and the algal biomass productivity were used as Key Performance Indicators.

In addition, the N_2O emission risk-factor was considered to spot unsuitable operation modes. Finally, a closer look at the biomass distribution among algae and bacteria biomasses was helpful to better interpret the evolution of the ecosystem.

3. Results and discussion

3.1. Model accuracy in predicting nitrogen removal rate and algal productivity

The model prediction capability for the most relevant monitored variables (pH, S_{O2}, S_{NH}, S_{NO3}, S_{NO2} and X_{ALG}) can be found in Casagli et al. [25],[26] (see also a summary in Supporting Information SI.1 and SI.2) and it covers an uncommonly broad range of conditions, including all the seasons, and HRT (=SRT) ranging from 2.6 to 20 days (see S.I.7).

The total ammoniacal nitrogen (TAN) removal rate (gN m^{-2} d^{-1}) and the Total Suspended Solids (TSS) productivity (gTSS m^{-2} d^{-1}) were also computed from the experimental measurements and compared to the model predictions (Fig. 2 and 3 for summer, autumn and winter, while spring results are shown in Supporting information, SI.4). It is worth

mentioning that algal productivity is rarely experimentally measured in algae-bacteria consortia, since only TSS or VSS (Volatile Suspended Solids) are monitored. Both turned out to be accurately predicted, as shown in Figure 1 and 2, with p-values for TSS productivity and TAN removal rate predictions below 1E-6. The highest TSS productivity was reached in summer, for both Narbonne and Milan, with an average value of 16.0 ± 5.6 [gTSS m^{-2} d^{-1}] (Summer 2018, Narbonne), 18.2 ± 2.0 [gTSS m^{-2} d^{-1}] (Summer 2019, Narbonne) and 12.2 ± 3.5 [gTSS m^{-2} d^{-1}] (Summer 2016, Milan).

During autumn and winter, the TSS productivity decreased in both experimentations, with an average value of 12.4 ± 3.1 and 12.7 ± 2.4 [gTSS m^{-2} d^{-1}] in autumn and winter, respectively, in Narbonne and of 6.1 ± 3.1 [gTSS m^{-2} d^{-1}] in autumn in Milan.

The generally higher values obtained in Narbonne along all the seasons are mainly due to the lower HRT, *i.e.* 5 days, (not considering the period where it was varied between 2.6 and 10, for days 240-253), compared to Milan (HRT = 10 -20 days), corresponding to a lower biomass harvesting rate. The TSS productivities shown in Figure 1a,b are in agreement with the experimental values reported in other literature works, where the raceways were operated under similar conditions. For instance, 10±6.5 gTSS m^{-2} d^{-1} [32]; 15.2±2.1 gTSS m^{-2} d^{-1} [33]; 5.5 ± 7.4 g TSS m^{-2} day^{-1} [34] ; 12.3 gTSS m^{-2} d^{-1} as maximum value during winter and 32.4 gTSS m^{-2} d^{-1} as maximum value during summer [35].

The model was further used to estimate the contributions from the different biomasses (X_{ALG}, X_{AOB}, X_{NOB}, X_H) and from inert and biodegradable compounds (X_I and X_S respectively) which all together make up the TSS.

Algae productivity in Milan represented 72% of the TSS productivity on a yearly basis (*i.e.* 7.03 gALG m^{-2} day^{-1} compared to 9.8 gTSS m^{-2} day^{-1}), corresponding to a microbial biomass ($X_{BIO} = X_{ALG}+X_{AOB}+ X_{NOB}+X_H$) composed by 90.4% of algae on yearly

average. For the Narbonne case study, algae productivity was 63% of the TSS productivity on a yearly bases (*i.e.* 9.5 gALG m^{-2} day^{-1} compared to 15.1 gTSS m^{-2} day^{-1}), corresponding to a microbial biomass where algae represented 76.6% of the community on yearly average.

Looking at TAN removal rate in Narbonne (Fig. 3), it was on average 0.4 ± 0.1 gN m^{-2} d^{-1} in summer, with HRT of 5 days. Peaks of 0.9 gN m^{-2} d^{-1} were reached at HRT of 10 days, while the lowest value was achieved for a HRT of 2.6 days (0.2 gN m^{-2} d^{-1}). In autumn and winter, the TAN removal rate was generally lower than 0.5 gN m^{-2} d^{-1}, due to the sub-optimal growth conditions for algae and bacteria. For the raceway located in Milan, the TAN removal rate was higher during summer, being in a range of 4.6-10.2 gN m^{-2} d^{-1} (average 6.9 ± 1.3) for a HRT of 10 days. In autumn, these values decreased, varying between 3.5-8.1 gN m^{-2} d^{-1} (average 4.9 ± 1.5), even when the HRT increased up to 20 days. The difference between the TAN removal rate in the two raceways is mainly due to differences in the influent nitrogen, both as concentration (8 gN m^{-3} in Narbonne and 310 gN m^{-3} on average in Milan) and as chemical nature (urea in Narbonne, and TAN in Milan). The TAN removal rates values are in agreement with the ranges reported in the work of Morillas-España et al. [36] (2.7 gN m^{-2} d^{-1} during winter and 4.3 gN m^{-2} d^{-1} during summer, for an inlet N-NH_4^+ concentration 168-210 g m^{-3}), for a raceway operated under similar HRT conditions (3-10 d).

In addition, the model allows assessing the fluxes of N-NH_3 stripped out and, therefore, computing the actual TAN removal rate (grey dotted line in Figure 2, a and b) by subtracting the contribution of the stripped N to the apparent TAN removal rate. In Milano, the imperfect pH regulation allowed going from pH 6.5 to 7.8 increasing the free NH_3 level by a factor of 30. Since TAN concentration was high in piggery digestate, this corresponded to large spikes of released NH_3. In Narbonne, the TAN concentration was

lower, but no pH regulation was implemented so that pH could even reach values above 10, resulting in temporarily high NH_3 fluxes as well.

a)

b)

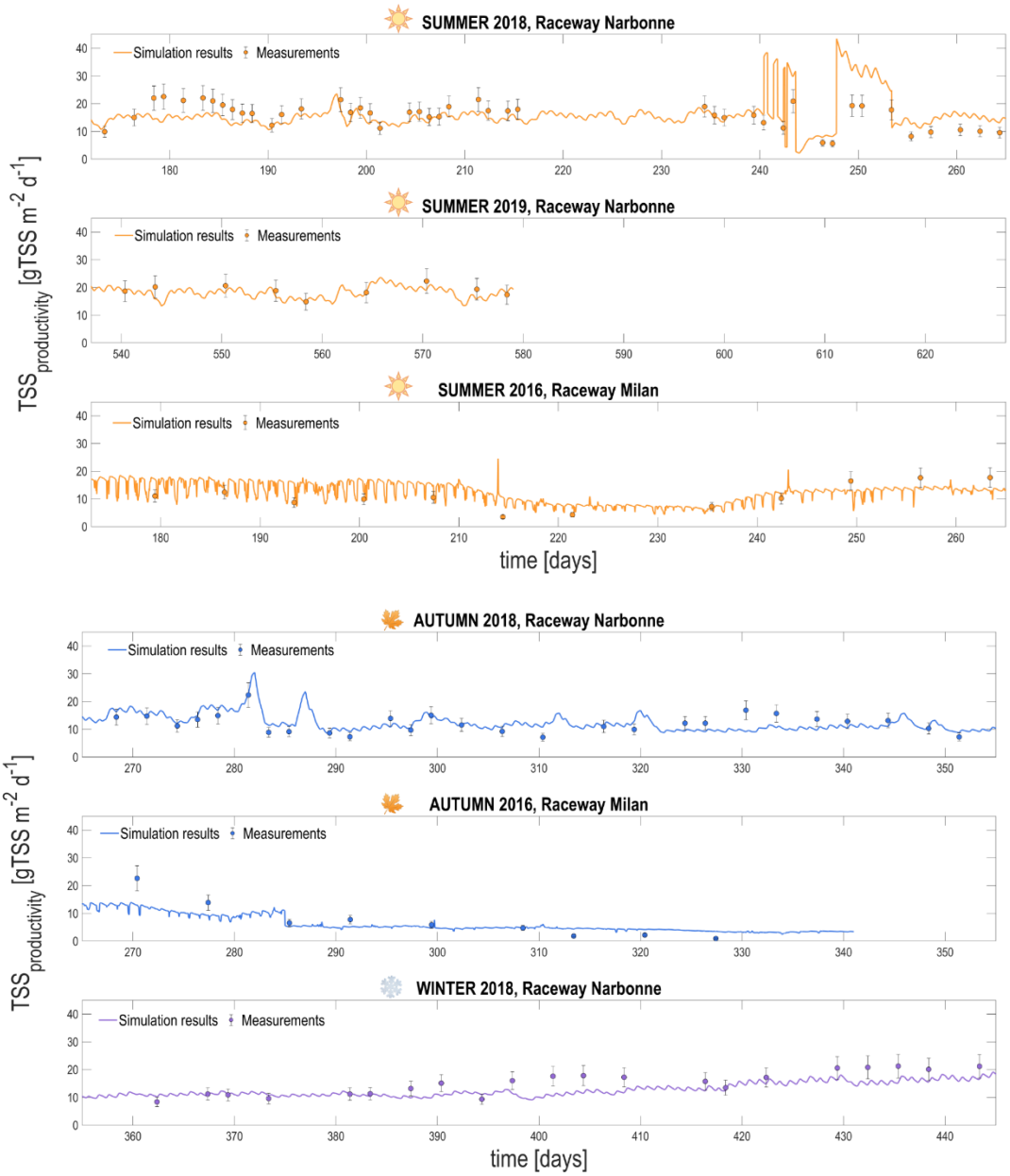

Figure 1. Total Suspended Solids productivity experimentally measured and computed with the ALBA model for Milan and Narbonne case studies according to the season (a: summer; b: autumn and winter).

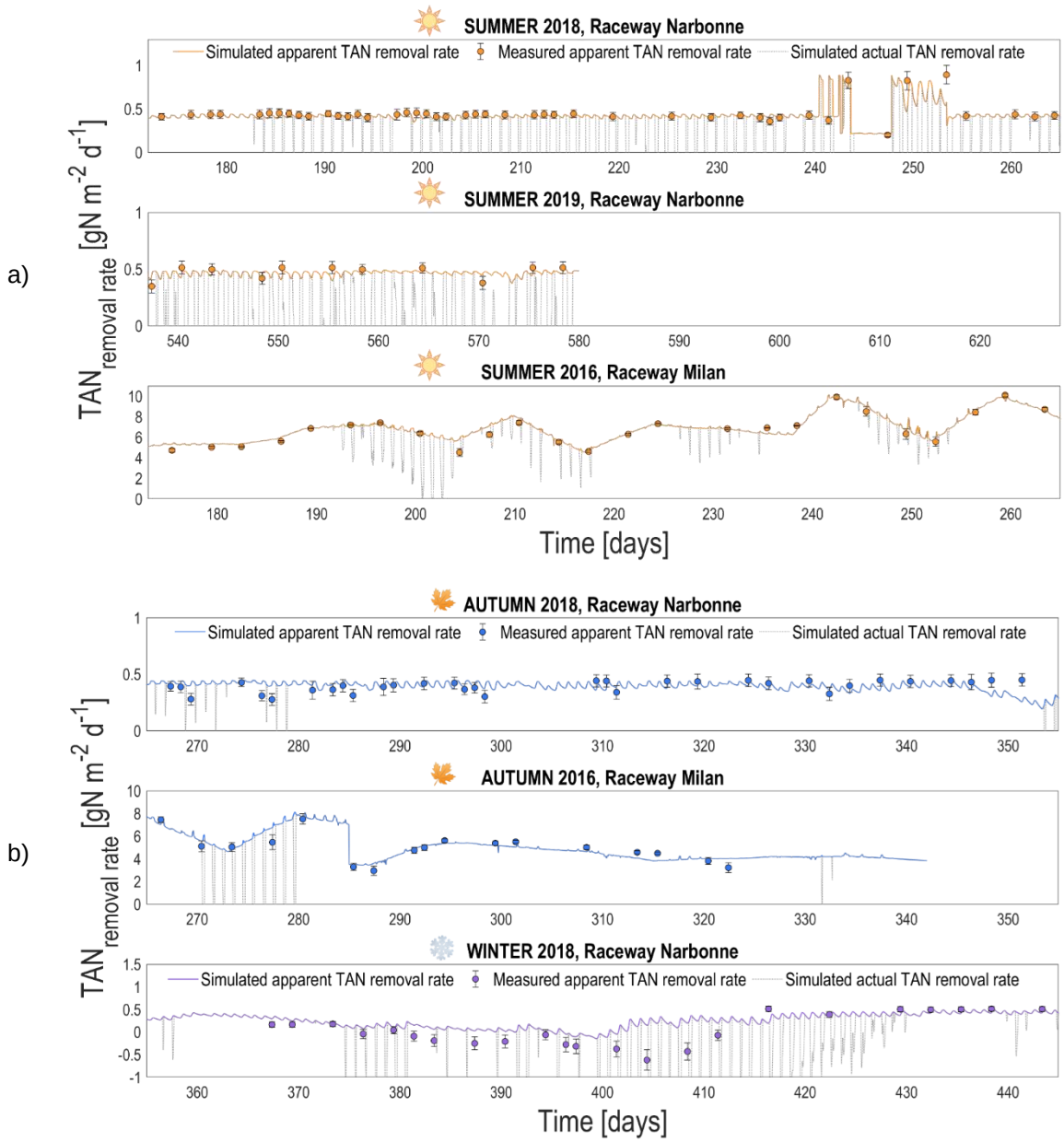

Figure 2. Total ammoniacal nitrogen removal rate, in gN m^{-2} d^{-1}, for both case studies (Milan and Narbonne) and according to seasons (a: summer; b: autumn and winter). The term apparent refers to the fact that the flux of N-NH_3 stripped out was considered as untreated nitrogen.

3.2. Model accuracy when uncoupling HRT and SRT

The experimental campaign of Robles et al. [19] , was used for validating the ALBA model when HRT is uncoupled from SRT. The experimental campaign was performed on the same outdoor pilot-scale raceway located in Narbonne, fed with synthetic municipal wastewater [37], previously used for the calibration and validation of the ALBA model [25]. The HRABP was operated with a liquid depth of 0.3 m and connected to a

high-flow industrial-scale membrane compartment. The authors evaluated the process performances computing the average biomass productivity and nitrogen removal rate over a 20 days experimental period, for each operational condition tested. Uncoupling SRT and HRT by membrane filtration improved process efficiency, with higher biomass throughput and nutrient removal rate at lower HRT operation. At an SRT of 6 days, the biomass productivity increased up to 19.9 ± 0.5 and to 28.5 ± 0.5 gVSS m^{-2} d^{-1} when HRT was set to 4 and 2.5 days, respectively. The corresponding nitrogen removal rates were 2.3 ± 0.4 and 3.3 ± 0.4 gN m^{-2} d^{-1}, respectively. The authors ran also an experiment with HRT set to 2.5 and SRT set to 6 days, but under sub-optimal light and temperature conditions, obtaining lower values for both biomass productivity and nitrogen removal rate (19.6 gVSS m^{-2} d^{-1} and 2.4 g N m^{-3} d^{-1}, respectively), compared to the experiment carried out with the same operational conditions and under optimal light and temperature ranges.

The ALBA model was run under the same operational conditions, considering the climatology of the year 2018-2019 [25]. Biomass productivity and nitrogen removal rate were computed according to Robles et al., [19] and simulation results were averaged on a seasonal time scale. Spring 2018 presented similar average light and temperature compared to the one reported by Robles et al. [19] as being optimal. The autumn climatology of 2018 turned out to be comparable to the light and temperature conditions reported as suboptimal by Robles et al. [19]. The model predictions, for both biomass productivity and nitrogen removal rate, are perfectly in agreement with the experimental results (Figure 3), with a R^2 of 0.78 and 0.93, respectively. Discrepancies between simulated and experimental data are mainly due to the dynamic temperature and light dataset used for simulations, that are not belonging to the same year as in Robles et al. [19], since these data were not available. Moreover, while in the work of Robles et al.

316 [19], the measurements were averaged on 20 days of experiments for each tested
317 condition, the simulated data were averaged on the entire season (3 months for spring
318 and 3 months for autumn).
319 These recorded (and simulated) biomass productivity and nitrogen removal rates are in
320 line with other experimental results obtained in different studies testing membrane
321 separation systems uncoupling HRT and SRT in outdoor algae-bacteria systems for
322 wastewater treatment (see Table 1 for a synthetic comparison of literature studies).
323 Morillas-España et al. [33] operated a 4.4 m^3 HRABP (surface 30 m^2, liquid depth 0.12
324 m) fed with primary domestic wastewater, at a constant SRT of 4.8 d and a variable HRT
325 of 4.8, 3.5, 2.6, 2 and 1.8 d, obtaining an algal productivity of 15.2, 17, 22.2, 22.6, 21.9
326 gDW m^{-2} d^{-1}, respectively. González-Camejo et al. [38] operated an outdoor membrane
327 photobioreactor (MPBR) of 5 m^2, treating tertiary sewage effluent, at HRT 1.5 d, SRT
328 4.5 d and liquid depth 0.25 m. They recorded an average biomass productivity of
329 15.7±1.4 gVSS m^{-2} d^{-1}. When operating the same system reducing the light path to 0.10
330 m and with HRT 4.5 d and SRT 3 d, the measured biomass productivity was 20±2.4
331 gVSS m^{-2} d^{-1} [39].
332 The simulation results of the ALBA model perfectly fall within these ranges proving its
333 prediction capacity under uncoupled HRT and SRT. Therefore, the model was further
334 used to run extensive simulations for investigating a wide set of scenarios.

A

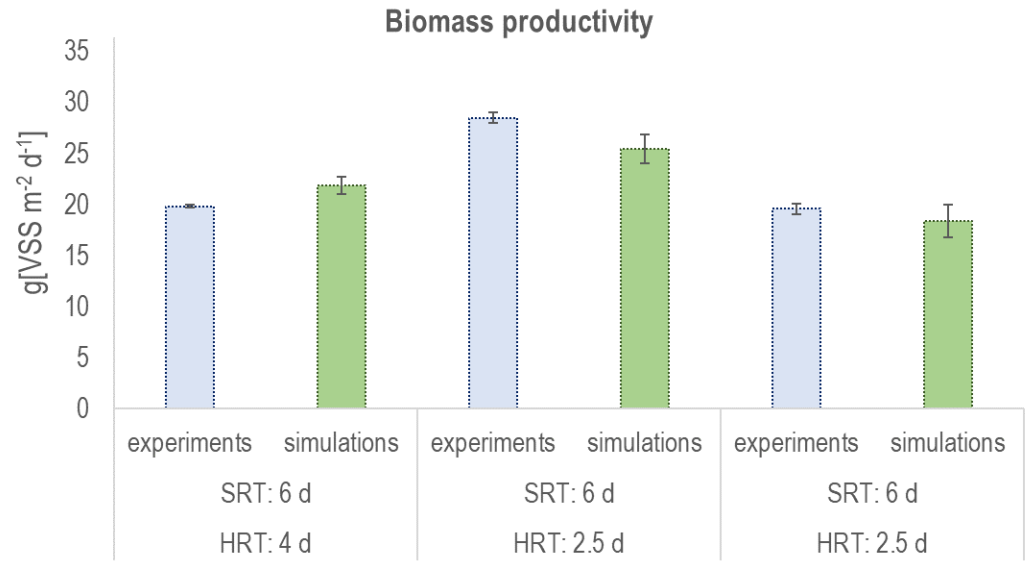

B

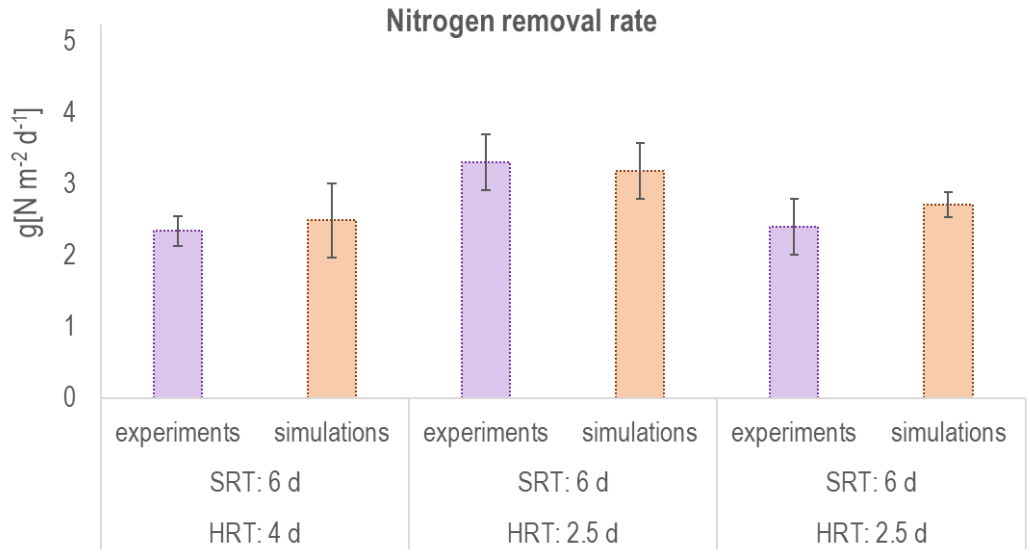

Figure 3. Comparison between experimental [19] and simulation results (this study) for HRT uncoupled from SRT. A) Biomass productivity, in gVSS m^{-2} d^{-1}; B) Nitrogen removal rate, in gN m^{-2} d^{-1}.

3.3. Best strategies to avoid GHG emissions: the key role of alkalinity

Simulations were run to explore optimal SRT and HRT for treating digestate. The (constant) liquid depth was set to 0.225 m, typical of raceways systems. The TA in the influent was set at its nominal value (10 mol m^{-3}), typical of a diluted digestate. Simulation outcomes are shown in Figure 4, while the 2D version of the graphs are reported in SI.5. As it was shown in Casagli et al. [26], despite pH regulation, a strong competition for inorganic carbon between algae and nitrifiers can take place since alkalinity is strongly reduced by nitrification. The consequence is a risk of N_2O emission that can be very detrimental to the environment. In fact, it turns out that the N_2O risk factor becomes nonzero for couples of HRT ≥ 4 d and SRT ≥ 2 d, reaching the highest values (35-45%) for HRT ≥ 8 d and SRT ≥ 4 d (Fig.4C).

The maximum of algal productivity (20.18 gAlg m^{-2} d^{-1}) was obtained for HRT=0.2 d and SRT=2 d (Fig.4A). This pair of hydraulic and solid retention times is not risky as for N_2O emission (risk factor is 0%). However, looking at the algae concentration and the efficiency in nitrogen recycling, both values are low (280 gCOD m^{-3} and 0.34% respectively, see Fig.4B and 4D). Indeed, for this low HRT, the nitrogen loading rate is high, leading to low efficiency of nitrogen recycling ($Eff_{N,Recyc}$). Very low SRT, typically lower than 1 d, whatever the HRT, lead to algal washout, with algal biomass concentration that goes to zero and so does the algal biomass productivity (Fig.4A and 4D). The maximum value for the efficiency in nitrogen recycling (10.4%) is obtained for a very different operational regime, i.e. HRT=10 d and SRT=3 d (Fig.4B). However, these conditions are associated to an unsustainable N_2O risk factor of 30% (Fig.4C). The higher algae and nitrifying bacteria concentrations, indeed lead to the exhaustion of the inorganic carbon pool. In addition, the algal productivity related to the highest efficiency in nitrogen recycling is reduced to 12.4 gAlg m^{-2} d^{-1}. This opposite trend

reflects a classical contrasting tendency between productivity and efficiency in nutrient use, like for the nitrogen removal rate and removal efficiency in wastewater remediation. This explains the conflicting trend for the Key Process Indicators (2.4.1 and 2.4.2).

Finally, the best operational conditions in terms of HRT and SRT for reaching a better trade-off between algae productivity and nitrogen recycling, while avoiding the risk of N_2O emission, appear to be when HRT ranges from 2 to 5 d and SRT from 2 to 3 d. However, under these conditions, the efficiency of nitrogen recycling is never higher than 6.6% (see Fig.4A and 4B).

In order to provide a better picture of the gain achievable by uncoupling HRT and SRT, Figure 5 reports a comparison between the algal productivity and the efficiency in nitrogen recycling when no solid/liquid separation is applied (*i.e.* HRT=SRT). In this case, HRT is adapted according to SRT, in order to maximize either algal productivity or nitrogen recycling efficiency. Figure 5A clearly shows that higher algae productivity are achieved for all the SRT values between 2 and 10 days, when operating the system with an HRT of 0.2 days. A doubling in algal productivity can be obtained by appropriately modulating HRT compared to the reference case of SRT=HRT. Figure 5B shows that the same is valid for the nitrogen recycling efficiency, that reaches higher values when these two operational parameters are decoupled (imposing HRT 10 days at varying SRT between 2 and 10 days). Nitrogen recycling efficiency could be tripled compared to the standard case when HRT=SRT.

Additional simulations were also run, by increasing the influent TA from 10 up to 15, 17.5, 20 and 22.5 mol m^{-3} (see Table SI.6.1 in SI.6). For an influent alkalinity increased up to 15 and 17.5 mol m^{-3}, inorganic carbon limiting conditions can still be reached when applying HRT ≥ 6 d and SRT ≥ 4 d, with a maximum value of N_2O risk factor of 45% for HRT=10 d and SRT=5, 6 and 7 d. On the contrary, with 20 and 22.5 mol m^{-3} of influent

TA, the N_2O risk factor is always zero, indicating that this level of alkalinity (0.90 and 1.02 mol molNH_4^{+-1} respectively, corresponding to 2.51 and 2.82 g$CaCO_3$ gNH_4^{+-1}) is adequate to fully support both algae and nitrifiers carbon request.

TA supplementation appears to be particularly beneficial for algae-bacteria systems when the aim is to treat wastewater, since it allows to set higher HRT and SRT, favouring: i) slow growers, such as AOB and NOB; ii) the inorganic carbon availability to guarantee the full nitrification process, simultaneously avoiding the competition with algae; iii) reduced NH_3 stripping conditions due to the improved TAN removal (see Fig.7D1 and 7D2) and, thus, lower TAN concentration in the reactor. The environmental benefit of this strategy is therefore evident.

It must be highlighted that alkalinity addition should be adjusted carefully to avoid a marked increase in CO_2 emissions due to overloading the system with inorganic carbon, especially when the pH in the raceway is controlled with CO_2 bubbling. Ideally, it should be regulated according to the CO_2 saturation level in the pond, that is strictly related to water temperature. In fact, the driving-force in the gas-liquid exchange is given by the difference between the gas saturation level in the liquid phase and the actual concentration of the dissolved gas. With TA addition, the buffering capacity of the system increases, and so does the level of soluble inorganic carbon. The risk is that when an external source of CO_2 is injected in the system for pH regulation, most of it is lost to the atmosphere.

When considering simultaneously the algal biomass productivity and the nitrogen recycling optimization, the situation does not change significantly. Regulating TA avoids N_2O emissions, but it does not allow to simultaneously reach these two conflicting objectives.

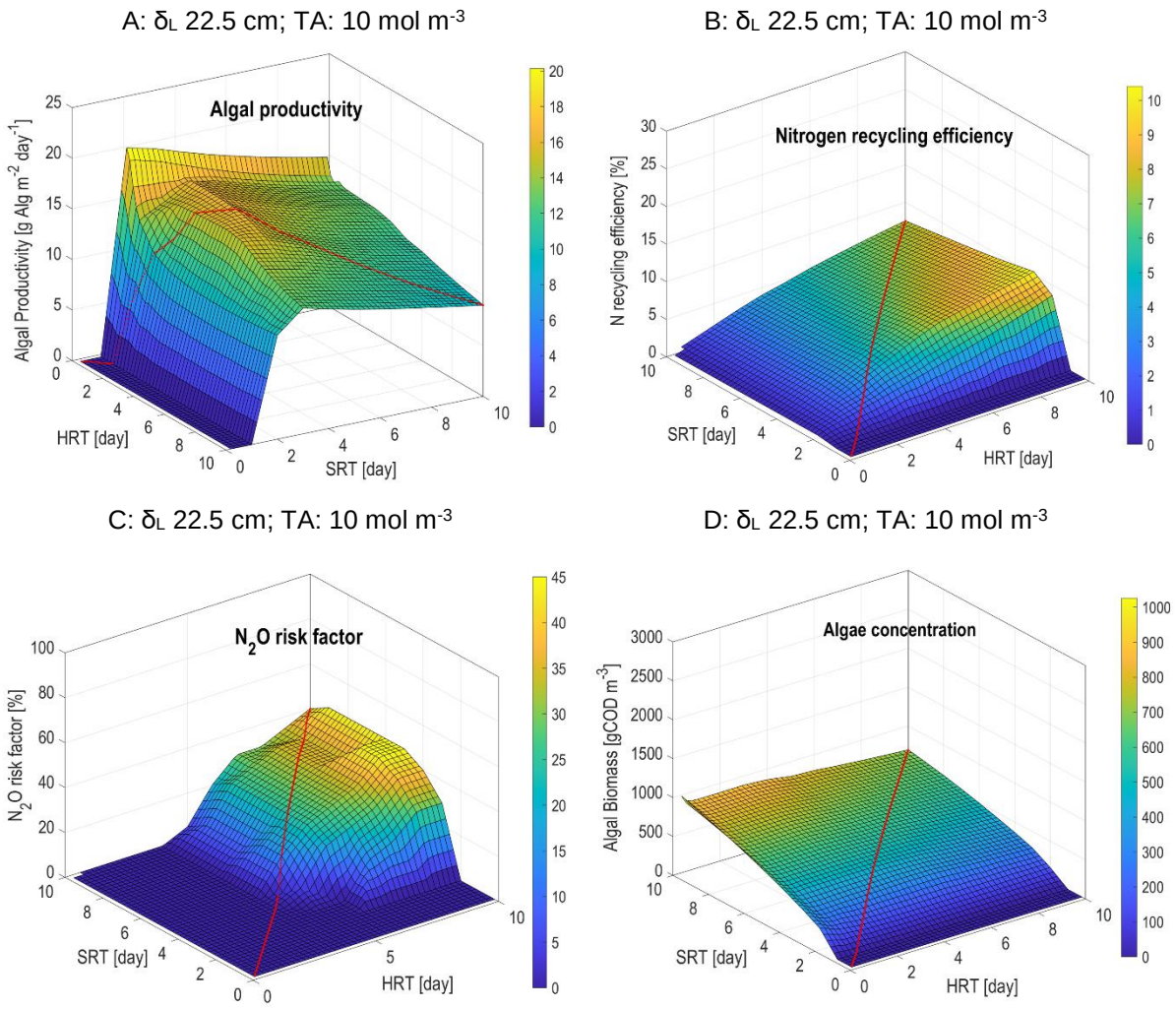

412 **Figure 4.** Simulation results at varying HRT (0.2-10 d) and SRT (0.2-10 d). Influent TA is 10 mol m^{-3} and depth, δ_L,
413 is 0.225 m. A: algal biomass productivity [gAlg m^{-2} d^{-1}]; B: Nitrogen recycling efficiency in the algal biomass [%]; C:
414 N_2O risk factor (percentage of time along the day for which N_2O formation conditions occur, *i.e.* inorganic carbon <
415 0.2 molC m^{-3}), [%]; D: Algal biomass concentration in the reactor [gCOD m^{-3}]. The red line represents the scenario
416 with no solid/liquid separation (*i.e.* HRT = SRT).
417
418

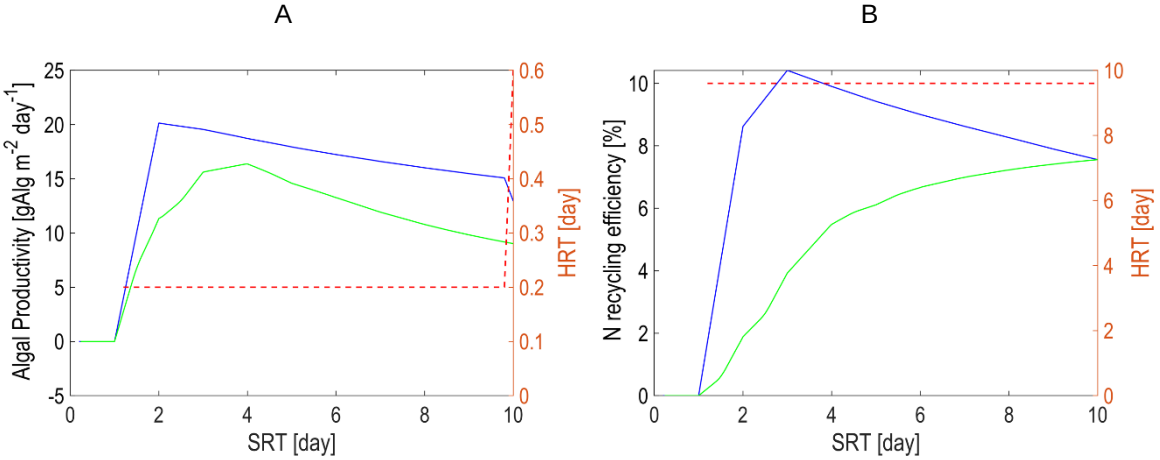

419 **Figure 5.** Simulation results for TA=10 mol m^{-3} and δL=0.225 m, comparing the scenario with no
420 solid/liquid separation (*i.e.* HRT=SRT, green continuous line) and the scenario where HRT (red dotted
421 line) is adapted according to the SRT in order to maximize: A) algal productivity [gAlg m^{-2} d^{-1}] and B)
422 nitrogen recycling efficiency [%], (blue continuous line).

3.4. Unravelling the influence of liquid depth

Two additional sets of simulations where run, considering the liquid depths of 0.12 and 0.06 m, first with the nominal alkalinity in the influent (10 mol m^{-3}). Results are shown in Figure 6.

For δ_L=0.12 m, the maximum of algal productivity is 19.4 gAlg m^{-2} d^{-1} for HRT=0.2 d and SRT=2 d (Fig. 6A), which is slightly lower than for the nominal depth (δ_L=0.225m) for the same HRT and SRT. The corresponding concentration of nitrogen recycled in the algal biomass is doubled (0.6%, Fig. 6B). Indeed, at constant HRT, the incoming nitrogen load per surface unit is lower for lower depth, while the incoming nitrogen load per volume unit is constant. The lower areal productivity, even if the algal concentration in the reactor is higher (Fig.7 A1), is due to the lower flowrate Q_{OUT}, necessarily associated to a lower δ_L for the same HRT, eventually resulting in a lower algal effluent flow rate. For this pair of HRT-SRT values, there is no risk of N_2O emission, but the nitrogen recycling efficiency is still very low.

The maximum nitrogen recovered as algae biomass (11.8%) is obtained for HRT=10 d and SRT=3 d, but for this pair of values the N_2O risk factor is 35% (Fig. 6B and 6C). So far, the best working range of both HRT and SRT, for guarantying elevated algal biomass productivity and efficiency in nitrogen recycling is 2-5 d, similarly to the case δ_L=0.225m. In comparison, the nitrogen uptake from the algal biomass is higher and the best trade-off between algal biomass productivity (15.25 gAlg m^{-2} d^{-1}) and nitrogen recycling (7.03%), avoiding N_2O favourable conditions, is obtained for HRT=3 d and SRT=5 d.

Decreasing δ_L to 0.06 m (assumed to be the lowest operational depth for this kind of systems), the maximum of algal biomass productivity (15.2 gAlg m^{-2} d^{-1}) is obtained for

448 HRT=1 d and SRT=6 d (Fig. 6D), with a corresponding nitrogen recycling of 4.7% (Fig.
449 6E) and algae concentration in the reactor of 2603 gCOD m^{-3} (see Fig. 9A1). Compared
450 to the the two-fold depth (δ_L=0.12 m), the maximum productivity is lower, even if the
451 algal concentration is almost 5 times higher. This is due to a much lower nutrient influent
452 load for 6 cm of liquid depth. Correspondingly, the nitrogen uptake in the algal biomass
453 is higher. In addition, under this condition of HRT and SRT, the N_2O risk factor is 0%
454 (Fig. 6F). The best result for nitrogen recycling efficiency (12.4%) was found for HRT=10
455 d and SRT=3 d, but it corresponds to a N_2O risk factor of 45% (Fig. 6F).
456 Finally, for this low liquid depth competition for inorganic carbon is stronger. It results
457 that the N_2O emission risk appears for a wider range of cases compared to δ_L=0.12 m.
458 In fact, while every value between 2 and 10 d can be applied for the SRT, the HRT
459 should stay lower than 1 d, or being increased: i) up to 7, imposing SRT=2 d; ii) up to 3,
460 imposing SRT=3 d; iii) up to 2, imposing SRT=4-5 d.
461 Additional simulations were run increasing the influent TA (see Figure 7 and 8), in order
462 to see the coupled effect of working at low liquid depth without alkalinity shortage in the
463 reactor.
464 Indeed, the TA influent addition allows to explore a wider range of HRT and SRT
465 (proportionally to the alkalinity added) without operating under inorganic carbon
466 limitation. This allows finding a much better trade-off between algal productivity and
467 nitrogen recycling efficiency. Total alkalinity must be at least 20 mol m^{-3}, to guaranty that
468 the N_2O risk factor is zero (Fig. 7C) for all HRT and SRT values.
469 Figure 8A and B show more explicitly which is the advantage for algal production and
470 nitrogen recycling respectively, when decoupling HRT and SRT, compared to the
471 scenario without membrane separation application. Adapting the HRT for each SRT

472 value can lead to a threefold increase in algal productivity or in the nitrogen recycling
473 rate.
474

475 **3.5. Analysis of the optimal regimes**

476 Figure 9 summarizes those conditions maximising algae productivity (left column) and
477 nitrogen recycling (right column), for three liquid depths (δ_L: 0.22, 0.12 and 0.06 m).
478 Algae and heterotrophic bacteria are indeed favoured (see Fig.9 A1) for the HRT-SRT
479 pair that maximise the algae productivity (HRT 0.2 d, SRT 2d, δ_L 0.22 and 0.12 m), while
480 nitrifying bacteria are washed-out from the system. Nonetheless, even if algae
481 productivity reaches higher values, between 18 and 21 gAlg m^{-2} d^{-1} (Fig.9 B1), the
482 corresponding nitrogen recycling remains below 1% (Fig.9 C1). The biomass
483 composition drastically changes for HRT 1d, SRT 6 d and δ_L 0.06 m. Algae are more
484 concentrated (with a concentration factor, compared to δ_L 0.12 and 0.22 m, ranging
485 between 5 and 9.5, respectively), and nitrifying bacteria reach concentrations
486 comparable to those of heterotrophic bacteria (Fig.9 A1). In this case, the corresponding
487 algae productivity is slightly lower (15 gAlg m^{-2} d^{-1}), due to the decreased harvesting
488 rate. However, the associated nitrogen recycling is higher (4.7%, see Fig.9 C1),
489 suggesting this operational configuration as the best trade-off between algae
490 productivity and nitrogen recycling when the target objective is the algae productivity.
491 The beneficial effect of increasing the influent alkalinity is mostly evident for TAN
492 removal rate (Fig.9 D1), that is always higher than 10 gN m^{-2} d^{-1} (reaching 22.6 gN m^{-2}
493 d^{-1} when operating at δ_L 0.22 m), compared to the cases where alkalinity was not added.
494 Also looking at the TAN removal rate in Fig.9 D1, the best trade-off when maximizing
495 algae productivity remains to operate the system at 0.06 m depth, HRT 1 d and SRT 3

d, since there is not a substantial difference comparing the TAN removal rate at 0.12 or 0.06 m.

The biomass composition reported in Fig.9 A2, shows how the HRT-SRT pair maximizing the nitrogen recycling in the algal biomass (10 and 3 d, respectively) favour algae and nitrifying bacteria, while heterotrophic bacteria concentration remains low. The highest algae productivity (14.3 gAlg m^{-2} d^{-1}, see Fig.9 B2) is obtained with alkalinity addition for δ_L 0.22 m, also corresponding to the highest TAN removal rate (6.9 gN m^{-2} d^{-1}, Fig.9 D2), while the best nitrogen recycling is reached for δ_L 0.06 m and with TA addition (Fig. 9C2). Results reported in Fig.9 A2, B2, C2 and D2 suggest that the best trade-off between algae productivity and nitrogen recycling, when the objective target is the nitrogen recycling, by operating the system at δ_L 0.22 m and with TA influent addition. Therefore, by analysing in detail the cluster of conditions maximizing algae productivity and nitrogen recycling among the tested conditions, we can conclude that operating with HRT≤1 d and SRT≤6 d allows reaching the highest values of algae production, while operating at HRT 10 d and SRT 3 d allows maximising the nitrogen recovery in the algal biomass (up to 15%). Given the opposite trends of these two targets, the best trade-off is to run the system at lower liquid depth (0.06 m) when the target is maximising the algal productivity, while operating with higher liquid depth (0.12-22 m) when the objective is to maximize the nitrogen recycled in the algae.

Moreover, results highlighted that working at lower liquid depth allows: i) to maintain a higher algal biomass concentration in the reactor (requiring less energy for algae harvesting), with comparable biomass productivity; ii) to prevent massive growth of both heterotrophic and nitrifying bacteria, that can compete with algae for the main nutrients [43].

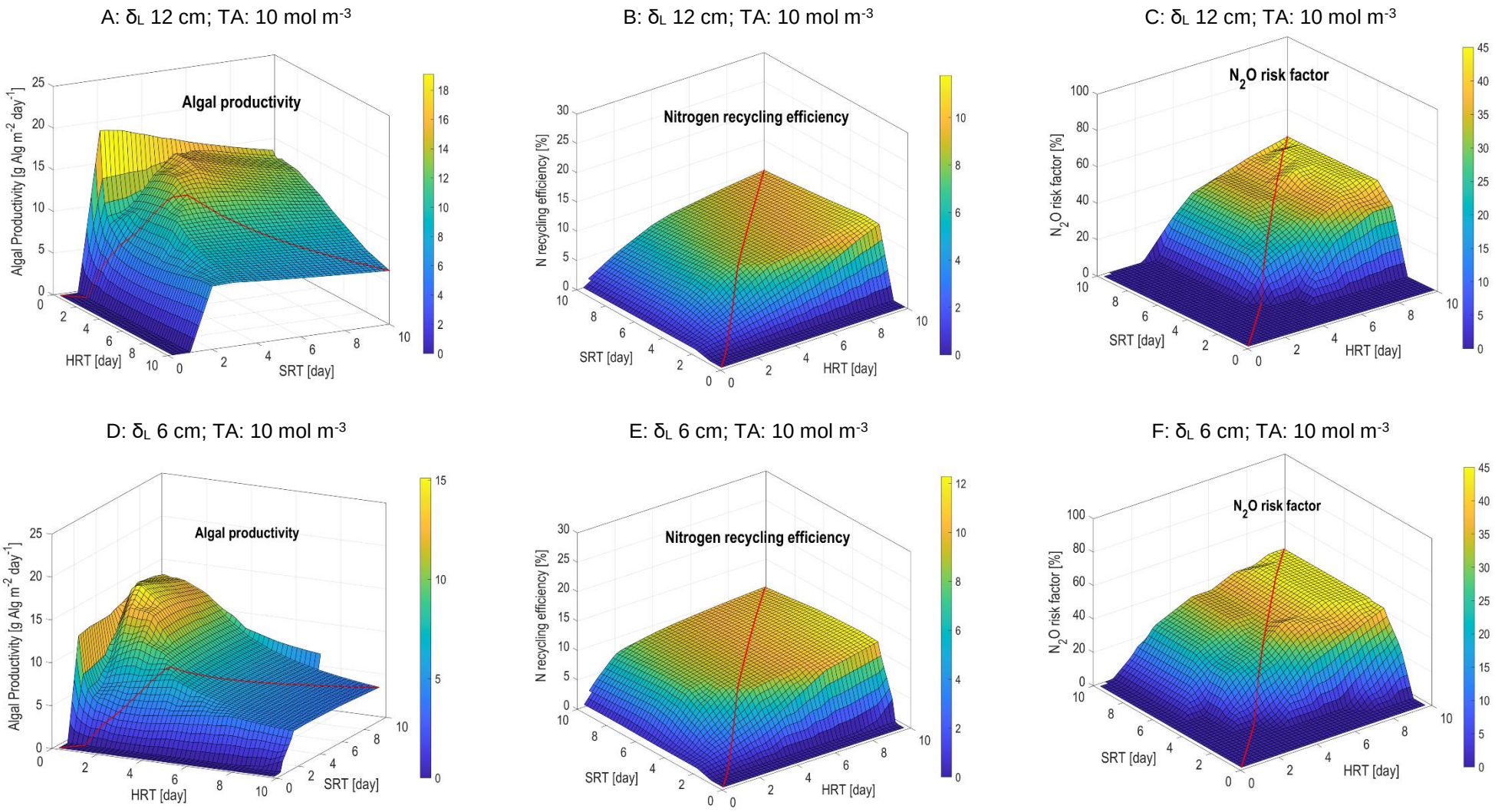

Figure 6. Simulation results at varying HRT (0.2-10 d) and SRT (0.2-10 d); influent TA (10 mol m^{-3}) and δ_L (0.12 m, A, B and C; 0.06 m, D, E and F). A, D: algal biomass productivity [gAlg m^{-2} d^{-1}]; B, E: Nitrogen recycling efficiency in the algal biomass [%]; C, F: N_2O risk factor (percentage of time along the day for which N_2O formation conditions occur, *i.e.* inorganic carbon < 0.2 molC m^{-3}), [%]. The red line represents the scenario with no solid/liquid separation (*i.e.* HRT = SRT).

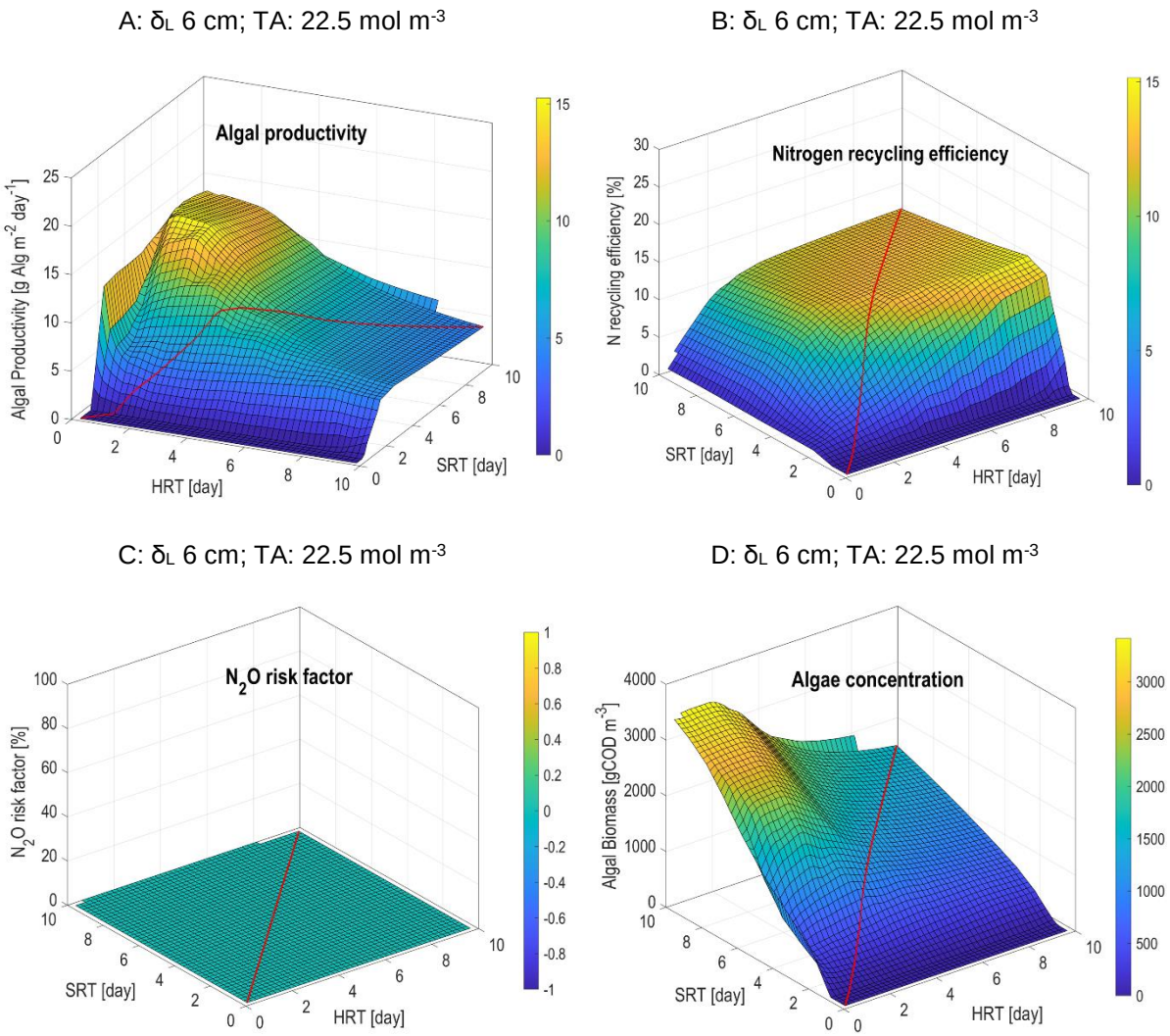

524 **Figure 7.** Simulation results at varying HRT (0.2-10 d) and SRT (0.2-10 d); influent TA (22.5 mol m^{-3}) and δL (0.06
525 m). A: algal biomass productivity [gAlg m^{-2} d^{-1}]; B: Nitrogen recycling efficiency in the algal biomass [%]; C: N_2O
526 risk factor (percentage of time along the day for which N_2O formation conditions occur, *i.e.* inorganic carbon < 0.2
527 molC m^{-3}), [%]; D: Algal biomass concentration in the reactor [gCOD m^{-3}]. The red line represents the scenario
528 with no solid/liquid separation (*i.e.* HRT = SRT).
529
530

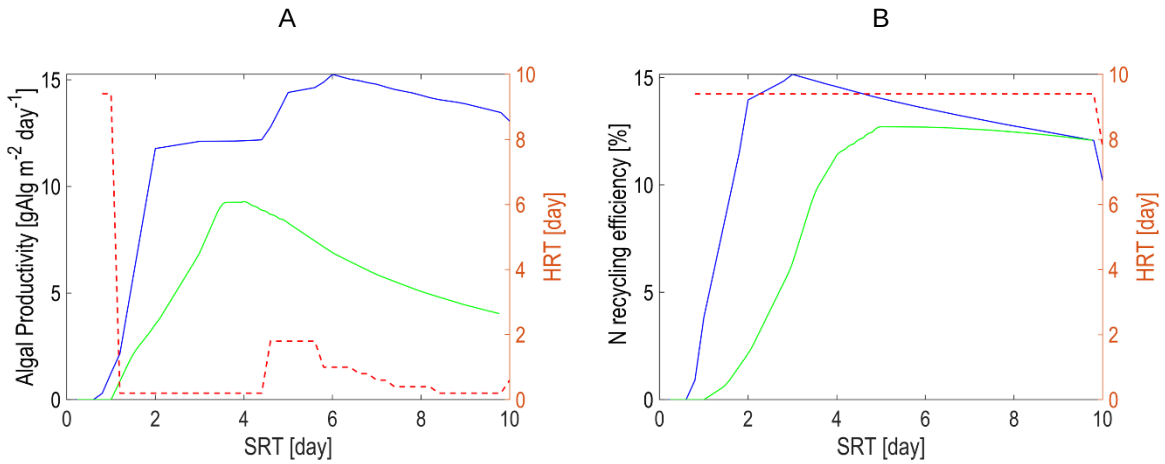

531 **Figure 8.** Simulation results for influent TA=22.5 mol m^{-3} and δL=0.06 m, comparing the scenario with
532 no solid/liquid separation (*i.e.* HRT=SRT, green continuous line) and the scenario where the HRT (red

dotted line) is adapted according to the SRT in order maximize: A) the algal productivity [gAlg m^{-2} d^{-1}] and B) the nitrogen recycling efficiency [%], (blue continuous line).

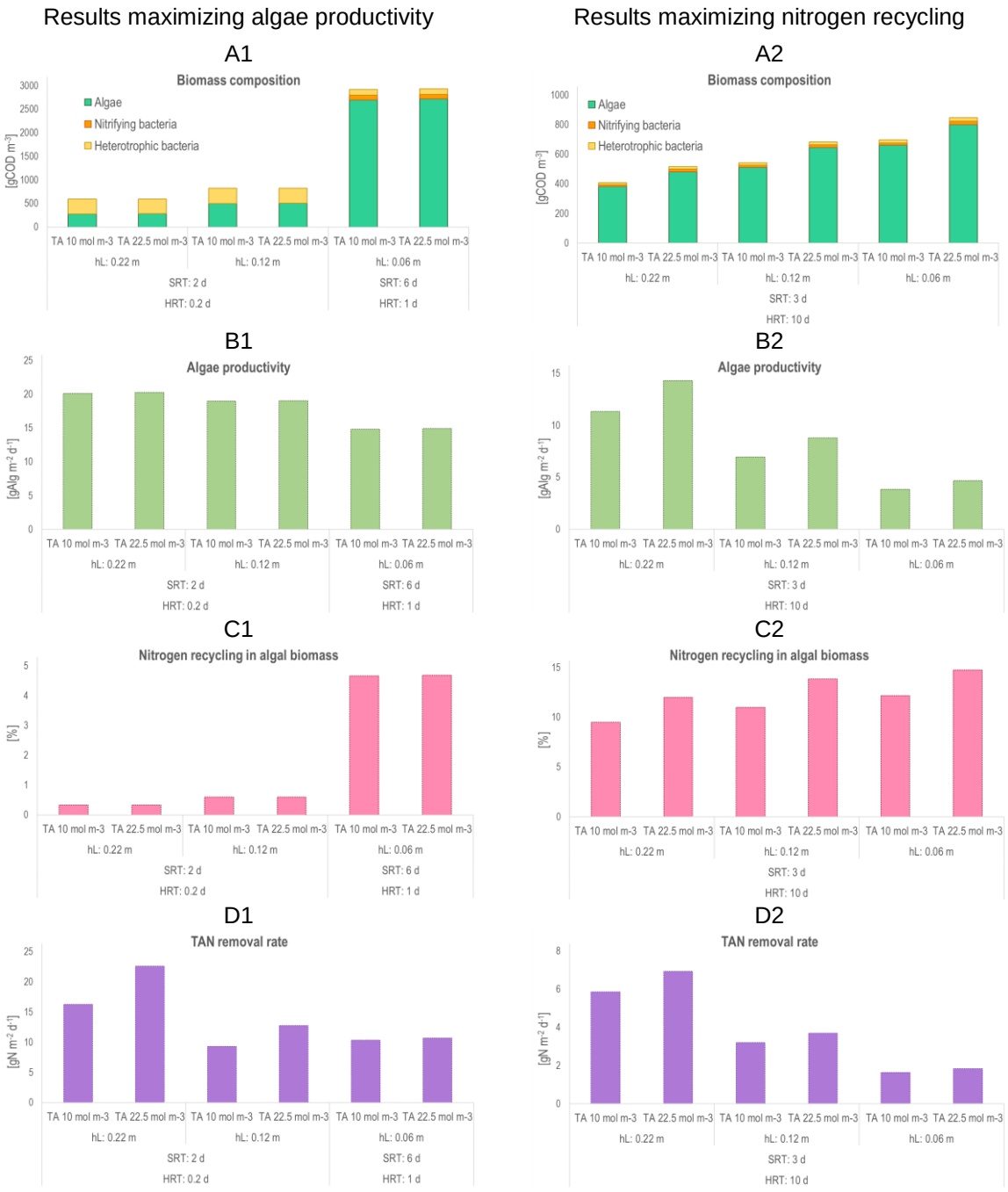

Figure 9. Simulation results for the conditions (HRT, SRT and δ_L) maximizing algae productivity (left column) and nitrogen recycling (right column). Results are given for both nominal (10 mol m^{-3}) and increased influent alkalinity (22.5 mol m^{-3}). A, B: biomass composition [gCOD m^{-3}]; C,D: algal biomass productivity [gAlg m^{-2} d^{-1}]; E,F: Nitrogen recycling in the algal biomass [%]; G,H: TAN removal rate [gN m^{-2} d^{-1}].

3.6. Further step to target emerging contaminants

Microalgae can play a role in the treatment of emerging contaminants by bioadsorption, bioaccumulation and metabolic degradation [18]. There is currently no efficient mathematical model validated in outdoor conditions describing such processes. It is even likely that models should be molecule-specific to be accurate. However, the ALBA model predicts the oxygen concentration in the medium, which gives an index of the intensity of the oxidative stress influencing the molecular degradation [17]. Simulation results showed that, under the tested conditions, oxygen concentration could reach pics up to 22 $mgO_2.L^{-1}$ during the day. A modelling study can be further carried out, imposing as target objective to maximise the peaks of oxygen concentration in the reactor, also by exploring a wider range of HRT and SRT values. The model can therefore indirectly predict the benefit in terms of emerging contaminant removal due to oxidative stress. Further work must be carried out to quantify these aspects, and further integrate it with an estimation of the gain in emerging contaminants treatment with a separation system. This is an important point when computing the cost-benefit of the separation system.

As recently reviewed by You et al. [44], pollutants (including pesticides, metals, engineered nanomaterials, pharmaceutical and personal care products, and aromatic pollutants) affect both bacteria and algae by interfering with their relationships. Cell-to-cell adhesion, substrate exchange and biodegradation of organic pollutants, enhancement of signal transduction, and horizontal transfer of tolerance genes are defence strategies in algal-bacterial systems, which should be further tamed and applied in wastewater treatment systems. Enhancing the treatment capacity by continuous addition of more efficient algae and/or bacteria

565 species is then the next step. This complementary strategy of bioaugmentation
566 could be combined to the separation system to further enhance the process
567 performance. Numeric simulations can guide the process optimization and
568 development for this new and promising strategy.
569

570 **3.7. Long-term membrane application for algae bacteria systems**

571 Membranes allow to decouple HRT and SRT and thus enhance the process
572 performance by more than 20%, with the possibility of recovering the algal biomass
573 for valuable applications [8].
574 However, membrane biofouling due to heavy suspended solids load, the small size
575 of microalgae and their poor sedimentation properties, combined with bacteria and
576 exopolymeric substances can lead to a progressive decline in the permeate flux
577 and an increase in the energy demand for operating the process, thus limiting long
578 term operations [41],[42]. Most of the membrane designs were developed for
579 wastewater treatment [43],[44], with very different objectives, such as removal of
580 pollutants and recovery of clean permeate vs recovery of valuable algal biomass
581 [42],[45]. The traditional fouling control techniques could be inefficient when
582 targeting a by-product recovery [45] and new directions have emerged in recent
583 years, while algal production was coupled to wastewater treatment [46]. Different
584 fouling control techniques have been developed recently, supported by a better
585 understanding of the interactions between the foulants and membrane surfaces.
586 The main strategies consist in changing the operating conditions, in pre-treating the
587 feed (using coagulation, adsorption, or oxidation), in mechanically cleaning of the
588 membranes, and in modifying the membrane surfaces by coatings or blending with
589 polymers and nanoparticles [45]. Choosing the adequate membrane cleaning

mechanism is of major importance in terms of energy consumption, permeate production, and overall process performance [46],[47]. The development of membranes for algae-bacteria systems with excellent bioactivity and associated to antifouling strategies is of crucial importance for long term applications.

Conclusion

This study showed the complexity and challenges for optimizing outdoor HRABP featured with solid/liquid separations systems, pointing out that the efficiency in nitrogen recycling and the algal productivity cannot be maximized simultaneously. Thus, it is fundamental to first choose the target of the process (e.g. wastewater remediation, algal productivity, emerging contaminant treatment…), which will then be reached by decoupling HRT and SRT: a gain of 23% on algal productivity (up to 20.3 $g.m^{-2}.day^{-1}$), and of 35% in nitrogen recycling could be obtained for the specific case study. When combined with depth optimization and alkalinity addition, nitrogen recycling rate can reach 15%, with an algal productivity staying above 16 $g.m^{-2}.day^{-1}$ thus offering an interesting trade-off. Long-term application of efficient membrane modules, and the characterisation of their efficiency on emerging contaminant treatment, will then be crucial for future implementation of these strategies.

Acknowledgments

OB, FC and FB benefited from the support of the ADEME Biomsa project. EF wish to thank the Fondazione Cariplo (project: Polo delle Microalghe) for their financial support.

Author contribution statements

FC developed the modified model with feedback from OB. FC and OB implemented the simulation framework. FC wrote the manuscript with permanent feedback from OB. EF, FB and OB guided FC in the definition of the case study framework. FB and OB obtained grants to support the study and supervised the work. In general, all authors provided critical feedback and helped shape the research, analysis and manuscript.

References

[1] Gonçalves, A. L. , Pires, J. C. M. , and Simões, M. A review on the use of microalgal consortia for wastewater treatment. *Algal Research* **2017**, 24, 403–415.

[2] Wang, M. , Keeley, R. , Zalivina, N. , Halfhide, T. , Scott, K. , Zhang, Q. , Steen, P. van der , and Ergas, S. J. Advances in algal-prokaryotic wastewater treatment: A review of nitrogen transformations, reactor configurations and molecular tools. *Journal of Environmental Management* **2018**, 217, 845–857.

[3] Lee, I. , Lim, H. , Jung, B. , Colosimo, M. F. , and Kim, H. Evaluation of aeration energy saving in two modified activated sludge processes. *Chemosphere* **2015**, 140, 72–78.

[4] Di Caprio, F. , Tayou Nguemna, L. , Stoller, M. , Giona, M. , and Pagnanelli, F. Microalgae cultivation by uncoupled nutrient supply in sequencing batch reactor (SBR) integrated with olive mill wastewater treatment. *Chemical Engineering Journal* **2021**, 410, 128417.

[5] Lage, S. , Gojkovic, Z. , Funk, C. , and Gentili, F. G. Algal Biomass from Wastewater and Flue Gases as a Source of Bioenergy. *Energies* **2018**, 11, 664.

[6] Shahid, M. K. , Kashif, A. , Fuwad, A. , and Choi, Y. Current advances in treatment technologies for removal of emerging contaminants from water – A critical review. **2021**

[7] Sutherland, D. L. and Ralph, P. J. 15 years of research on wastewater treatment high rate algal ponds in New Zealand: discoveries and future directions. *New Zealand Journal of Botany* **2020**, 58, 334–357.

[8] Sutherland, D. L. and Ralph, P. J. Microalgal bioremediation of emerging contaminants - Opportunities and challenges. *Water Research* **2019**, 164, 114921.

[9] Yang, Y. , Ok, Y. S. , Kim, K.-H. , Kwon, E. E. , and Tsang, Y. F. Occurrences and removal of pharmaceuticals and personal care products (PPCPs) in drinking water and water/sewage treatment plants: A review. *Science of The Total Environment* **2017**, 596–597, 303–320.

[10] Bai, X. , Lutz, A. , Carroll, R. , Keteles, K. , Dahlin, K. , Murphy, M. , and Nguyen, D. Occurrence, distribution, and seasonality of emerging contaminants in urban watersheds. *Chemosphere* **2018**, 200, 133–142.

[11] Teodosiu, C. , Gilca, A.-F. , Barjoveanu, G. , and Fiore, S. Emerging pollutants removal through advanced drinking water treatment: A review on processes and environmental performances assessment. *Journal of Cleaner Production* **2018**, 197, 1210–1221.

[12] Rempel, A. , Biolchi, G. N. , Antunes, A. C. F. , Gutkoski, J. P. , Treichel, H. , and Colla, L. M. Cultivation of Microalgae in Media Added of Emergent Pollutants and Effect on Growth, Chemical Composition, and Use of Biomass to Enzymatic Hydrolysis. **2021**

[13] Vale, F. , Sousa, C. A. , Sousa, H. , Santos, L. , and Simões, M. Impact of parabens on microalgae bioremediation of wastewaters: A mechanistic study. *Chemical Engineering Journal* **2022**, 442, 136374.

[14] Ding, T. , Wang, S. , Yang, B. , and Li, J. Biological removal of pharmaceuticals by Navicula sp. and biotransformation of bezafibrate. *Chemosphere* **2020**, 240, 124949.

[15] Ding, T. , Yang, M. , Zhang, J. , Yang, B. , Lin, K. , Li, J. , and Gan, J. Toxicity, degradation and metabolic fate of ibuprofen on freshwater diatom Navicula sp. *Journal of Hazardous Materials* **2017**, 330, 127–134.

[16] Matamoros, V. , Uggetti, E. , García, J. , and Bayona, J. M. Assessment of the mechanisms involved in the removal of emerging contaminants by microalgae from wastewater: a laboratory scale study. *Journal of Hazardous Materials* **2016**, 301, 197–205.

[17] Matamoros, V. , Gutiérrez, R. , Ferrer, I. , García, J. , and Bayona, J. M. Capability of microalgae-based wastewater treatment systems to remove emerging organic contaminants: a pilot-scale study. *Journal of Hazardous Materials* **2015**, 288, 34–42.

[18] Rempel, A. , Gutkoski, J. P. , Nazari, M. T. , Biolchi, G. N. , Cavanhi, V. A. F. , Treichel, H. , and Colla, L. M. Current advances in microalgae-based bioremediation and other technologies for emerging contaminants treatment. *The Science of the Total Environment* **2021**, 772, 144918.

[19] Robles, Á. , Capson-Tojo, G. , Gales, A. , Viruela, A. , Sialve, B. , Seco, A. , Steyer, J.-P. , and Ferrer, J. Performance of a membrane-coupled high-rate algal pond for urban wastewater treatment at demonstration scale. *Bioresource Technology* **2020**, 301, 122672.

[20] Yunlong , Luo , Pierre , Le-Clech , K, R. , and Henderson Simultaneous microalgae cultivation and wastewater treatment in submerged membrane photobioreactors: A review. *Algal research* **2017**

[21] Marbelia, L. , Bilad, M. R. , Passaris, I. , Discart, V. , Vandamme, D. , Beuckels, A. , Muylaert, K. , and Vankelecom, I. F. J. Membrane photobioreactors for integrated microalgae cultivation and nutrient remediation of membrane bioreactors effluent. *Bioresource Technology* **2014**, 163, 228–235.

[22] Sousa, C. A. , Sousa, H. , Vale, F. , and Simões, M. Microalgae-based bioremediation of wastewaters - Influencing parameters and mathematical growth modelling. *Chemical Engineering Journal* **2021**, 425, 131412.

[23] Sánchez-Zurano, A. , Guzmán, J. L. , Acién, F. G. , and Fernández-Sevilla, J. M. An Interactive Tool for Simulation of Biological Models Into the Wastewater Treatment With Microalgae. *Frontiers in Environmental Science* **2021**, 9

[24] Pessoa, R. W. S. , Mendes, F. , Oliveira, T. R. , Oliveira-Esquerre, K. , and Krstic, M. Numerical optimization based on generalized extremum seeking for fast methane production by a modified ADM1. *Journal of Process Control* **2019**, 84, 56–69.

[25] Casagli, F. , Zuccaro, G. , Bernard, O. , Steyer, J.-P. , and Ficara, E. ALBA: A comprehensive growth model to optimize algae-bacteria wastewater treatment in raceway ponds. *Water Research* **2021**, 190, 116734.

[26] Casagli, F. , Rossi, S. , Steyer, J. P. , Bernard, O. , and Ficara, E. Balancing Microalgae and Nitrifiers for Wastewater Treatment: Can Inorganic Carbon Limitation Cause an Environmental Threat? *Environmental Science & Technology* **2021**, 55, 3940–3955.

[27] Plouviez, M. and Guieysse, B. Nitrous oxide emissions during microalgae-based wastewater treatment: current state of the art and implication for greenhouse gases budgeting. *Water Science and Technology* **2020**, 82, 1025–1030.

[28] Baar, H. J. W. de Von Liebig's law of the minimum and plankton ecology (1899–1991). *Progress in Oceanography* **1994**, 33, 347–386.

[29] Batstone, D. J. , Keller, J. , Angelidaki, I. , Kalyuzhnyi, S. V. , Pavlostathis, S. G. , Rozzi, A. , Sanders, W. T. M. , Siegrist, H. , and Vavilin, V. A. The IWA Anaerobic Digestion Model No 1 (ADM1). *Water Science and Technology* **2002**, 45, 65–73.

[30] Henze, M. , Gujer, W. , Mino, T. , and Loosedrecht, M. van Activated Sludge Models ASM1, ASM2, ASM2d and ASM3. *Water Intelligence Online* **2000**, 5, 9781780402369–9781780402369.

[31] Pizzera, A. , Scaglione, D. , Bellucci, M. , Marazzi, F. , Mezzanotte, V. , Parati, K. , and Ficara, E. Digestate treatment with algae-bacteria consortia: A field pilot-scale experimentation in a sub-optimal climate area. *Bioresource Technology* **2019**, 274, 232–243.

[32] Rossi, S. , Pizzera, A. , Bellucci, M. , Marazzi, F. , Mezzanotte, V. , Parati, K. , and Ficara, E. Piggery wastewater treatment with algae-bacteria consortia: Pilot-scale validation and techno-economic evaluation at farm level. *Bioresource Technology* **2022**, 351, 127051.

[33] Morillas-España, A. , Sánchez-Zurano, A. , Lafarga, T. , Morales-Amaral, M. del M. , Gómez-Serrano, C. , Acién-Fernández, F. G. , and González-López, C. V. Improvement of wastewater treatment capacity using the microalga Scenedesmus sp. and membrane bioreactors. **2021**

[34] Mantovani, M. , Marazzi, F. , Fornaroli, R. , Bellucci, M. , Ficara, E. , and Mezzanotte, V. Outdoor pilot-scale raceway as a microalgae-bacteria sidestream treatment in a WWTP. *Science of The Total Environment* **2020**, 710, 135583.

[35] Sánchez-Zurano, A. , Morillas-España, A. , Gómez-Serrano, C. , Ciardi, M. , Acién, G. , and Lafarga, T. Annual assessment of the wastewater treatment capacity of the microalga Scenedesmus almeriensis and optimisation of operational conditions. *Scientific Reports* **2021**, 11, 21651.

[36] Morillas-España, A. , Lafarga, T. , Sánchez-Zurano, A. , Acién-Fernández, F. G. , Rodríguez-Miranda, E. , Gómez-Serrano, C. , and González-López, C. V. Year-long evaluation of microalgae production in wastewater using pilot-scale raceway photobioreactors: Assessment of biomass productivity and nutrient recovery capacity. *Algal Research* **2021**, 60, 102500.

[37] Nopens, I. , Capalozza, C. , and Vanrolleghem, P. A. Stability analysis of a synthetic municipal wastewater. **2001**, 23.

[38] González-Camejo, J. , Jiménez-Benítez, A. , Ruano, M. V. , Robles, A. , Barat, R. , and Ferrer, J. Optimising an outdoor membrane photobioreactor for tertiary sewage treatment. *Journal of Environmental Management* **2019**, 245, 76–85.

[39] González-Camejo, J. , Aparicio, S. , Jiménez-Benítez, A. , Pachés, M. , Ruano, M. V. , Borrás, L. , Barat, R. , and Seco, A. Improving membrane photobioreactor performance by reducing light path: operating conditions and key performance indicators. *Water Research* **2020**, 172, 115518.

[40] Viruela, A. , Robles, Á. , Durán, F. , Ruano, M. V. , Barat, R. , Ferrer, J. , and Seco, A. Performance of an outdoor membrane photobioreactor for resource recovery from anaerobically treated sewage. *Journal of Cleaner Production* **2018**, 178, 665–674.

[41] Arbib, Z. , Godos, I. de , Ruiz, J. , and Perales, J. A. Optimization of pilot high rate algal ponds for simultaneous nutrient removal and lipids production. *Science of The Total Environment* **2017**, 589, 66–72.

[42] Parsy, A. , Bidoire, L. , Saadouni, M. , Bahuaud, M. , Elan, T. , Périé, F. , and Sambusiti, C. Impact of seasonal variations on Nannochloropsis oculata phototrophic productivity in an outdoor pilot scale raceway. *Algal Research* **2021**, 58, 102375.

[43] Chiaramonti, D. , Prussi, M. , Casini, D. , Tredici, M. R. , Rodolfi, L. , Bassi, N. , Zittelli, G. C. , and Bondioli, P. Review of energy balance in raceway ponds for microalgae cultivation: Re-thinking a traditional system is possible. *Applied Energy* **2013**, 102, 101–111.

[44] You, X. , Xu, N. , Yang, X. , and Sun, W. Pollutants affect algae-bacteria interactions: A critical review. *Environmental Pollution (Barking, Essex: 1987)* **2021**, 276, 116723.

[45] Novoa, A. F. , Vrouwenvelder, J. S. , and Fortunato, L. Membrane Fouling in Algal Separation Processes: A Review of Influencing Factors and Mechanisms. *Frontiers in Chemical Engineering* **2021**, 3

[46] Liao, Y. , Bokhary, A. , Maleki, E. , and Liao, B. A review of membrane fouling and its control in algal-related membrane processes. *Bioresource Technology* **2018**, 264, 343–358.

[47] Zhang, W. and Jiang, F. Membrane fouling in aerobic granular sludge (AGS)-membrane bioreactor (MBR): Effect of AGS size. *Water Research* **2019**, 157, 445–453.

[48] Zhang, W. , Liang, W. , Zhang, Z. , and Hao, T. Aerobic granular sludge (AGS) scouring to mitigate membrane fouling: Performance, hydrodynamic mechanism and contribution quantification model. *Water Research* **2021**, 188, 116518.

[49] Deng, L. , Guo, W. , Ngo, H. H. , Zhang, H. , Wang, J. , Li, J. , Xia, S. , and Wu, Y. Biofouling and control approaches in membrane bioreactors. *Bioresource Technology* **2016**, 221, 656–665.

[50] Fortunato, L. , Lamprea, A. F. , and Leiknes, T. Evaluation of membrane fouling mitigation strategies in an algal membrane photobioreactor (AMPBR) treating secondary wastewater effluent. *Science of The Total Environment* **2020**, 708, 134548.

[51] Zhao, Z. , Liu, B. , Ilyas, A. , Vanierschot, M. , Muylaert, K. , and Vankelecom, I. F. J. Harvesting microalgae using vibrating, negatively charged, patterned polysulfone membranes. *Journal of Membrane Science* **2021**, 618, 118617.